

An Extension of the Lyapunov Analysis for the Predictability Problem

G. BOFFETTA

Dipartimento di Fisica Generale, Università di Torino and INFN, Unità di Torino, Torino, Italy

P. GIULIANI AND G. PALADIN

Dipartimento di Fisica, Università dell'Aquila and INFN, Unità dell'Aquila, L'Aquila, Italy

A. VULPIANI

Dipartimento di Fisica, Università di Roma "La Sapienza," and INFN, Unità di Roma, Rome, Italy

(Manuscript received 12 May 1997, in final form 9 February 1998)

ABSTRACT

The predictability problem for systems with different characteristic timescales is investigated. It is shown that even in simple chaotic dynamical systems, the leading Lyapunov exponent is not sufficient to estimate the predictability time. This fact is due to the saturation of the error on the fast components of the system, which therefore do not contribute to the exponential growth of the uncertainty at large error levels. It is proposed to adopt a generalization of the Lyapunov exponent that is based on the natural concept of error growing time at fixed error size. The predictability time defined in terms of the finite size Lyapunov exponent displays a strong dependence on the error magnitude, as already recognized by other authors.

The method is first illustrated on a simple numerical model obtained by coupling two Lorenz systems with different timescales. As a more realistic example, the analysis is then applied to a "toy" model of the atmospheric circulation recently introduced by Lorenz.

1. Introduction

The prediction of the future state of a system knowing its initial conditions is a fundamental problem with obvious applications in geophysical flows (Leith 1971, 1975; Leith and Kraichnan 1972; Leith 1978; Dalcher and Kalnay 1987; Chen 1989; Farrell 1990). There are many limitations to the ability of predicting the state of a geophysical system, for example, the atmosphere; one of the most important is the lack of knowledge, or the difficulty of full implementation, of the equations of motion. Still, even if one assumes a perfect knowledge of the equation of motion and sufficiently large computers, the predictability can be severely limited by the dynamics itself, that is, the "intrinsic predictability" of a system, which is the subject of our study.

A well known, and very popular, example of a low predictable system is given by a chaotic system (Lorenz 1963). By definition, chaotic dynamical systems display sensitive dependence on initial conditions: two initially close trajectories will diverge exponentially in the phase

space with a rate given by the leading Lyapunov exponent λ_{\max} (see Eckmann and Ruelle 1985). Because the initial conditions can be measured only with a finite uncertainty δ , we can forecast the future state of the system at a tolerance level, Δ , only up to a maximum time,

$$T_p \sim \frac{1}{\lambda_{\max}} \ln \left(\frac{\Delta}{\delta} \right). \quad (1)$$

One important consequence of Eq. (1) is that the predictability time has a very weak dependence on the accuracy of the initial condition and on the tolerance; therefore the predictability time is an intrinsic quantity of the system just as the Lyapunov exponent is.

The naive formula (1) for the predictability time holds only for infinitesimal perturbations and in nonintermittent systems; in the general case one has a series of problems and subtle points that have been the object of several studies in the last years (Crisanti et al. 1993a,b; Aurell et al. 1996, 1997). One delicate issue is particularly relevant for our present study and essentially says that, although the Lyapunov exponent for the atmosphere (as a whole) is presumably rather large (due to the small-scale turbulence), the large-scale behavior of the system can be forecasted with good accuracy for

Corresponding author address: Guido Boffetta, Dipartimento di Fisica Generale, via P. Giuria 1, 10125 Torino, Italy.
E-mail: boffetta@to.infn.it

several days (Lorenz 1969; Lorenz 1982; Simmons et al. 1995).

The apparent paradox stems from the identification of the predictability time with the inverse of the Lyapunov exponent based on Eq. (1), which is actually of little relevance even in few-degree-of-freedom dynamical systems. Indeed, in the presence of different characteristic timescales, as is the case in any realistic model of geophysical flows, the Lyapunov exponent will be roughly proportional to the inverse smallest characteristic time. This time is associated to the smallest, low-energy-containing scales that, as soon as their error reaches the saturation, do not play a role any more in the error growth law. Large errors will grow, in general, with the characteristic time of the largest energy-containing scales (Leith 1971; Leith and Kraichnan 1972). Thus when the initial uncertainty is not very small, as is often the case in a predictability experiment, the leading Lyapunov exponent may play no role at all (Toth and Kalnay 1993).

To be more quantitative, in this paper we investigate the predictability problem in systems with two timescales. We apply a recently introduced generalization of the Lyapunov exponent to finite perturbations. We will show that the “finite size Lyapunov exponent” (FSLE) is more suitable for characterizing the predictability of complex systems, in which the growth rate of large errors is not ruled by the Lyapunov exponent.

The models considered here are crude approximations of a realistic geophysical flow also because both the subsystems (representing large-scale and small-scale dynamics) have a single timescale. It would be interesting to extend our investigation to more realistic situations and comparing the latter case with present results.

The remainder of the paper is organized as follows: in section 2 we introduce the finite size Lyapunov exponent, which is applied to the system models in section 3. Section 4 is devoted to conclusions.

2. The finite size Lyapunov exponent

The notion of the Lyapunov exponent is based on the average rate of exponential separation of two infinitesimally close trajectories in the phase space:

$$\lambda_{\max} = \lim_{t \rightarrow \infty} \lim_{\delta x(0) \rightarrow 0} \frac{1}{t} \ln \frac{\delta x(t)}{\delta x(0)}, \quad (2)$$

where $\delta x(t)$ is the distance between the trajectories with a suitable norm and the two limits cannot be interchanged. The standard algorithm (Benettin et al. 1980) for computing the Lyapunov exponent is based on (2), with the trick of a periodical rescaling of the two trajectories in order to keep their separation distance “infinitesimal.”

As already discussed in the previous section, the second limit in (2) is of dubious interest in the predictability problem because the initial uncertainty of the system

variables is in general not infinitesimal. Therefore one would like to relax the infinitesimal constraint, still maintaining some well-defined mathematical properties. Recently, a generalization of (2) that allows one to compute the average exponential separation of two trajectories at finite errors δ has been introduced (Aurell et al. 1997). The finite size Lyapunov exponent $\lambda(\delta)$ is based on the concept of error growing time $T_r(\delta)$, which is the time it takes for a perturbation of initial size δ to grow by a factor, r . The ratio r should not be taken too large, in order to avoid the growth through different scales. The error growing time is a fluctuating quantity and one has to take the average along the trajectory as in (2). The finite size Lyapunov exponent is then defined as

$$\lambda(\delta) = \left\langle \frac{1}{T_r(\delta)} \right\rangle_t \ln r = \frac{1}{\langle T_r(\delta) \rangle} \ln r, \quad (3)$$

where $\langle \dots \rangle_t$ denotes the natural measure along the trajectory and $\langle \dots \rangle$ is the average over many realizations. The second equality comes from the definition of the time average along a trajectory for a generic quantity, $A(t)$,

$$\langle A \rangle_t = \frac{1}{T} \int_0^T A(t) dt = \frac{\sum_i A_i \tau_i}{\sum_i \tau_i} = \frac{\langle A \tau \rangle}{\langle \tau \rangle} \quad (4)$$

in the particular case of $A = 1/\tau$ (Aurell et al. 1997).

In the limit of infinitesimal perturbations, $\delta \rightarrow 0$, definition (3) reduces to that of the leading Lyapunov exponent (2). In practice, $\lambda(\delta)$ displays a plateau at the value λ_{\max} for sufficiently small δ .

To practically compute the FSLE, one has first to define a series of thresholds, $\delta_n = r^n \delta_0$, and to measure the time $T_r(\delta_n)$ that a perturbation with size δ_n takes to grow up to δ_{n+1} . The time $T_r(\delta_n)$ is obtained by following the evolution of the perturbation from its initial size δ_{\min} up to the largest threshold δ_{\max} . This is done by integrating two trajectories of the system that start at an initial distance δ_{\min} . In general, one must take $\delta_{\min} \ll \delta_0$, in order to allow the direction of the initial perturbation to align with the most unstable direction in the phase space. The FSLE $\lambda(\delta_n)$ is then computed by averaging the error growing time over several realizations according to (3).

Note that the FSLE has conceptual similarities with the ϵ entropy. This latter measures the bandwidth that is necessary for reproducing the trajectory of a system within a finite accuracy δ . The ϵ -entropy approach has already been applied to the analysis of simple systems and experimental data (Gaspard and Wang 1993), giving interesting results. The calculation of the ϵ entropy is, however, much more expensive from a computational point of view and of little relevance for the predictability problem.

The computation of the FSLE gives information on the typical predictability time for a trajectory with initial uncertainty δ . To be more quantitative, we can introduce

the average predictability time for an initial error δ and a given tolerance, Δ , as the average error growing time, that is,

$$T_p = \int_{\delta}^{\Delta} \frac{d \ln \delta'}{\lambda(\delta')}, \quad (5)$$

which reduces to (1) in the case of constant λ . From general considerations, one expects that $\lambda(\delta)$ is a decreasing function of δ and thus (5) gives longer predictability time than (1).

3. The models

We now discuss the application of the FSLE analysis to two relatively simple dynamical systems presenting different characteristic timescales. The proposed models are of little physical relevance; they should rather be considered as prototypical models for the predictability problem in complex flows.

The first example is obtained by coupling two Lorenz models (Lorenz 1963), the first representing the slow dynamics and the second the fast dynamics:

$$\begin{cases} \frac{dx_1^{(s)}}{dt} = \sigma(x_2^{(s)} - x_1^{(s)}) \\ \frac{dx_2^{(s)}}{dt} = (-x_1^{(s)}x_3^{(s)} + r_s x_1^{(s)} - x_2^{(s)}) - \epsilon_s x_1^{(f)} x_2^{(s)} \\ \frac{dx_3^{(s)}}{dt} = x_1^{(s)} x_2^{(s)} - b x_3^{(s)} \\ \frac{dx_1^{(f)}}{dt} = c \sigma(x_2^{(f)} - x_1^{(f)}) \\ \frac{dx_2^{(f)}}{dt} = c(-x_1^{(f)} x_3^{(f)} + r_f x_1^{(f)} - x_2^{(f)}) + \epsilon_f x_1^{(f)} x_2^{(s)} \\ \frac{dx_3^{(f)}}{dt} = c(x_1^{(f)} x_2^{(f)} - b x_3^{(f)}). \end{cases} \quad (6)$$

The choice of the form of the coupling is constrained by the physical request that the solution remains in a bounded region of the phase space. Since

$$\begin{aligned} \frac{d}{dt} \left\{ \epsilon_s \left(\frac{(x_1^{(f)})^2}{2\sigma} + \frac{(x_2^{(f)})^2}{2} + \frac{(x_3^{(f)})^2}{2} - (r_f + 1)x_3^{(f)} \right) \right. \\ \left. + \epsilon_f \left(\frac{(x_1^{(s)})^2}{2\sigma} + \frac{(x_2^{(s)})^2}{2} + \frac{(x_3^{(s)})^2}{2} - (r_s + 1)x_3^{(s)} \right) \right\} < 0, \end{aligned} \quad (7)$$

if the trajectory is far enough from the origin, it will evolve in a bounded region of the phase space. The parameters have the values $\sigma = 10$, $b = 8/3$, and $c = 10$, the latter giving the relative timescale between fast and slow dynamics. The two Rayleigh numbers are taken differently, $r_s = 28$ and $r_f = 45$ for generality.

With the present choice, the two uncoupled systems ($\epsilon_s = \epsilon_f = 0$) display chaotic dynamics with Lyapunov

exponents $\lambda^{(f)} \approx 12.17$ and $\lambda^{(s)} \approx 0.905$, respectively, and thus a relative intrinsic timescale of order 10.

By switching on the couplings ϵ_s and ϵ_f we obtain a single dynamical system whose maximal Lyapunov exponent λ_{\max} is close (for small couplings) to the Lyapunov exponent of the faster decoupled system ($\lambda^{(f)}$). We will consider a single realization of the couplings, with $\epsilon_f = 10$ and $\epsilon_s = 10^{-2}$. The global Lyapunov exponent is found to be in this case $\lambda_{\max} \approx 11.5$, which is indeed close to $\lambda^{(f)}$ in the uncoupled case. With the present choice of the couplings, the fast dynamics is driven by means of the effective Rayleigh number $r_{\text{eff}} = r_f + \epsilon_f x_2^{(s)}(t)/c$ and one can recognize in the time evolution the slow-varying component of the driver (see Fig. 1).

With regard to predictability, one expects reasonably that for small coupling ϵ_s the slow component of the system x_s remains predictable up to its own characteristic time. On the other hand, for any coupling $\epsilon \neq 0$ we obtain a single dynamical system in which the errors grow with the leading Lyapunov exponent $\lambda_{\max} \approx \lambda^{(f)}$. The apparent paradox stems from saturation effects that become apparent as soon as one is interested in non-infinitesimal errors.

We have integrated two trajectories of (6) starting from very close initial conditions. One trajectory represents the “true” (reference) trajectory \mathbf{x} and the other is the forecast (perturbed trajectory \mathbf{x}') subjected to an initial error, $\delta\mathbf{x}(0)$. The error is computed here by means of the Euclidean distance in the phase space

$$\begin{aligned} \delta\mathbf{x}(t) &= (\delta x_f(t)^2 + \delta x_s(t)^2)^{1/2} \\ &= \left[\sum_{i=1}^3 (x_i^{(f)} - x_i^{(f)'})^2 + \sum_{i=1}^3 (x_i^{(s)} - x_i^{(s)'})^2 \right]^{1/2}. \end{aligned} \quad (8)$$

Figure 2 reports the results for the error growth, averaged over 500 experiments, with $\delta x_f(0) = 10^{-8}$ and $\delta x_s(0) = 10^{-12}$. We observe that the relative magnitude of the initial errors is irrelevant for what concerns small errors because the error direction in the phase space will be rapidly aligned toward the most unstable direction. For small times ($t \leq 2$), both the errors can be considered infinitesimal and the growth rate is thus given by the global Lyapunov exponent λ_{\max} . This is the linear regime for the error growth in which the Lyapunov exponent is the relevant parameter for the predictability. For larger times, the fast component of the error, δx_f , reaches the saturation; the trajectory separation evolves now according to the full nonlinear equations of motion and the growth rate for the slow component is strongly reduced. From Fig. 2 one observes that the slow component error δx_s is still well below its saturation value and grows with a rate close to its characteristic inverse time $\lambda^{(s)}$.

We now apply the FSLE algorithm to the slow component of the error, δx_s (Fig. 3). We define a series of $m = 25$ thresholds starting from $\delta_0 = 10^{-6}$ with ratio

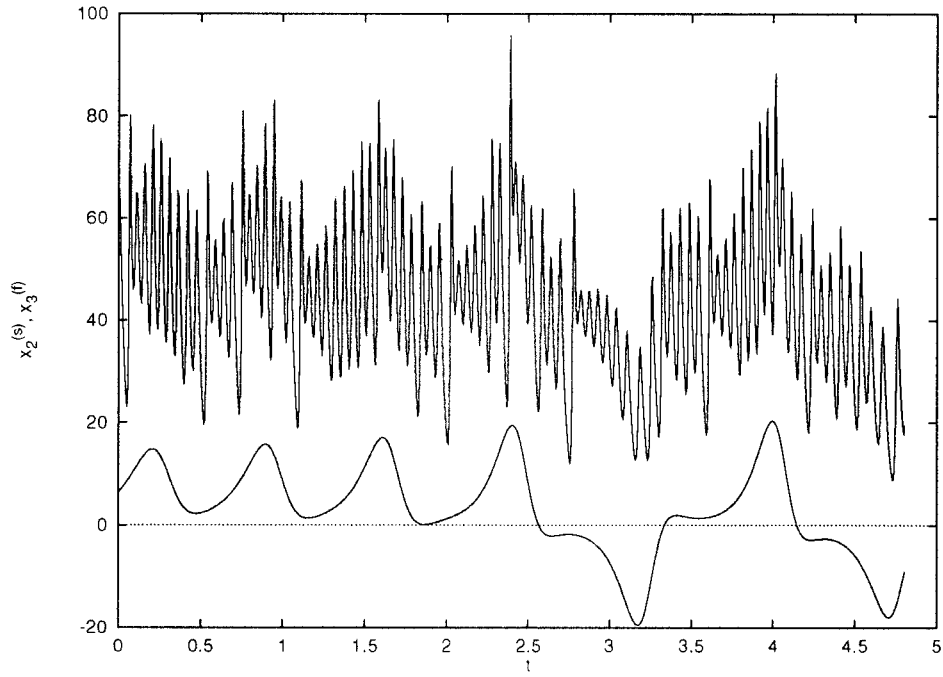


FIG. 1. Time series of the slow variable $x_2^{(s)}$ (lower curve) and of the fast variable $x_3^{(f)}$ (upper curve) on the attractor.

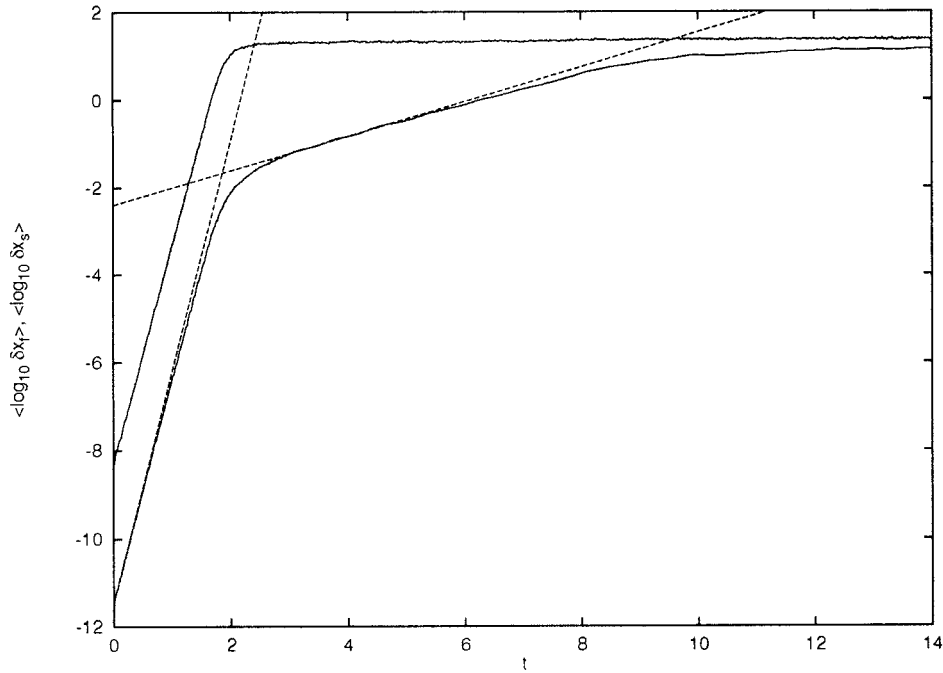


FIG. 2. Typical error growth for the fast component δx_f (upper curve) and for the slow component δx_s in the coupled Lorenz models with $\delta x_f(0) = 10^{-8}$ and $\delta x_s(0) = 10^{-12}$, averaged over 500 samples. In order to detect the typical behavior we compute the average of the logarithm. The dashed lines show the exponential growths with exponents $\lambda^{(f)}$ and $\lambda^{(s)}$.

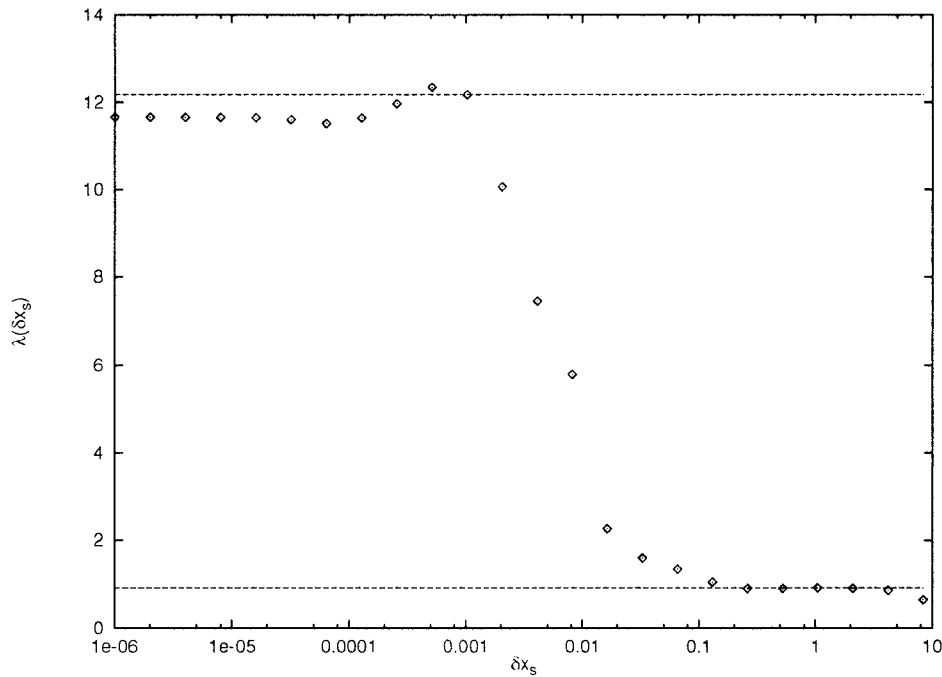


FIG. 3. FSLE for the two coupled Lorenz models computed from the slow variables. The parameters for the computation are $\delta_0 = 10^{-6}$, $m = 25$, $r = 2$, and $N = 500$. The two horizontal lines represent the uncoupled Lyapunov exponents $\lambda^{(f)}$ and $\lambda^{(s)}$.

$r = 2$. The results presented (Fig. 3) are obtained after averaging over $N = 500$ realizations. For very small δ , the FSLE recovers the leading Lyapunov exponent λ_{\max} , indicating that in small error predictability the fast component has indeed a dominant role. As soon as the error grows above the coupling ϵ_s , $\lambda(\sigma)$ drops to a value close to $\lambda^{(s)}$ and the characteristic time of the small-scale dynamics is no more relevant.

It is clear that the transition to the second regime [$\lambda(\delta) \approx \lambda^{(s)}$] is observable only if the coupling ϵ_s with the fast dynamics is smaller than the saturation value of the slow-component error. For large values of ϵ_s the fast-scale dynamics dominates the slow-scale dynamics and one observes a single predictability regime.

In Fig. 4 we plot the slow-component predictability time (5) for a fixed initial uncertainty $\delta x_s = 10^{-6}$ as a function of the tolerance Δ . We observe, as expected, an enhancement of T_p as soon as one accepts a tolerance larger than the typical fast component fluctuation in the slow time series. Observe that the application of (1) would heavily underestimate the predictability time for large tolerances (dashed line).

We now consider the second example. It is a more complex system recently introduced by Lorenz (Lorenz 1996) as a “toy” model for the atmosphere dynamics that includes explicitly both large scales (synoptic scales, slow component) and small scales (convective scales, fast component). The apparent paradox described above can be reformulated here by saying that an atmospheric model with fine spatial resolution (which is

able to capture the small-scale dynamics) would be less predictable than one with less spatial resolution (which resolves only large-scale motion) and thus the latter should be preferred for numerical weather forecasting. We will see that, also in this case, the effect of the small, fast-evolving scales becomes irrelevant for the predictability of large-scale motion if one considers large errors.

The model introduces a set of large-scale, slow-evolving variables x_k and small-scale, fast-evolving variables $y_{j,k}$ with $k = 1, \dots, K$ and $j = 1, \dots, J$. As in Lorenz (1996) we assume periodic boundary conditions on k ($x_{K+k} = x_k$, $y_{j,K+k} = y_{j,k}$), while for j we impose $y_{j,J+k} = y_{j,k+1}$. The equations of motion are

$$\begin{aligned} \frac{dx_k}{dt} &= -x_{k-1}(x_{k-2} - x_{k+1}) - x_k + F - \sum_{j=1}^J y_{j,k}, \\ \frac{dy_{j,k}}{dt} &= -cby_{j-1,k}(y_{j-2,k} - y_{j-1,k}) - cy_{j,k} + x_k, \end{aligned} \quad (9)$$

in which c represents again the relative timescale between fast and slow dynamics and b is a parameter that controls the relative amplitude.

Let us note that (9) has the same qualitative structure of a finite mode truncation of Navier–Stokes equations, with quadratic inertial terms and viscous dissipation. The coupling (with unit strength) is chosen in order to have the energy

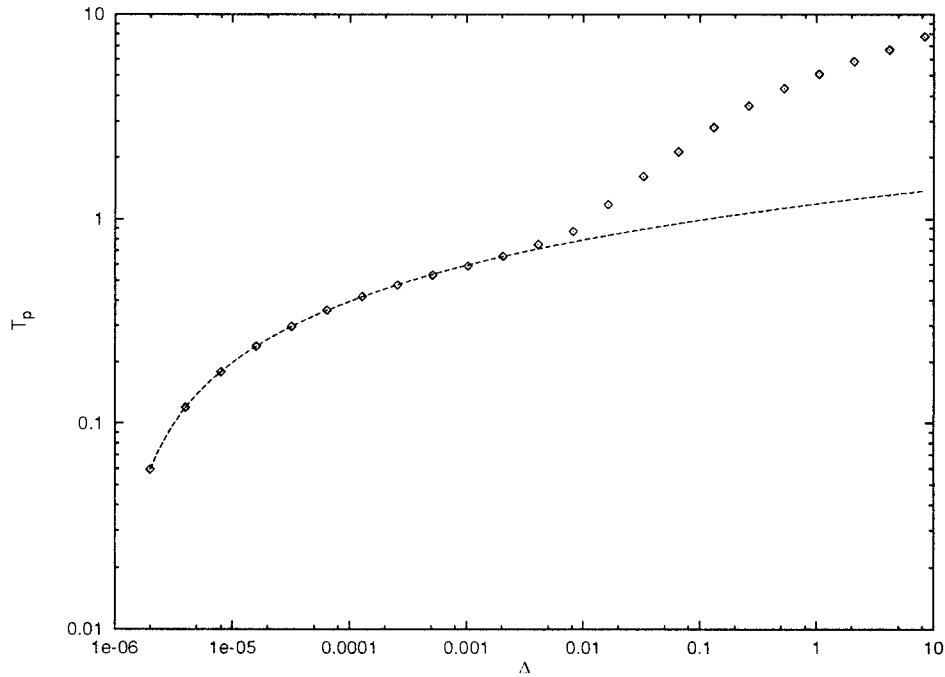


FIG. 4. Predictability time for the slow component of the two coupled Lorenz models as a function of the tolerance Δ . The initial error is fixed at $\delta = 10^{-6}$. The dashed line represents the Lyapunov estimation $T_p \sim \lambda^{-1} \ln(\Delta/\delta)$.

$$E = \frac{1}{2} \left(\sum_{k=1}^K x_k^2 + \sum_{k=1}^K \sum_{j=1}^J y_{j,k}^2 \right), \quad (10)$$

conserved in the inviscid, unforced limit. The forcing term drives only the large scales and we will consider the case $F = 10$, which is sufficient for developing chaos.

We have performed the computation of the FSLE for the system (9) with parameters as in Lorenz (1996): $K = 36, J = 10, c = b = 10$, which imply that the typical y variable is 10 times faster and smaller than the x variable. In this case we choose to adopt for measuring the error the global Euclidean norm on both the slow and fast variables (energy norm): this is to mimic a realistic situation in which we are not able to recognize a priori the slow component in the system.

The result of the FSLE computation is displayed in Fig. 5 after the average over $N = 1000$ realizations with initial error $\delta_{\min} = 10^{-5}$. We set $m = 20$ thresholds with $\delta_0 = 10^{-3}$ and ratio $r = 2^{1/2}$. For very small errors we observe the saturation of $\lambda(\delta)$ to the leading Lyapunov exponent of the system $\lambda_{\max} \approx 9.9$. For errors larger than the typical rms value of the fast variables ($\langle y^2 \rangle^{1/2} \approx 0.25$) we observe a second plateau at $\lambda \approx 0.5$, corresponding to the inverse characteristic time of large scales. We observe that the relative timescale between fast and slow motions as computed by the FSLE is slightly larger than the value of the parameter c . We think that this effect is due to coupling, which cannot here be assumed small as in the previous example.

In Fig. 6 we plot the predictability time (5) for fixed initial uncertainty $\delta = 10^{-3}$ and different tolerances. As in the previous example, we find an enhancement of the predictability time for large tolerances Δ with respect to the Lyapunov exponent estimation. For large initial errors (as it is usually the case in numerical weather forecasting) the predictability time is thus independent of the Lyapunov exponent.

4. Conclusions

We have shown that in systems that possess different characteristic timescales, the predictability time can be independent of the leading Lyapunov exponent. The latter is usually associated with the faster characteristic time and dominates the exponential growth of infinitesimal errors. Large errors will evolve, in general, with the large-scale characteristic time, which thus governs large error predictability.

We have introduced a generalization of the Lyapunov exponent that allows one to compute the average exponential error growth at a given error size, δ . The finite size Lyapunov exponent (FSLE) is expected to converge to the leading Lyapunov exponent for very small errors. For larger errors, $\lambda(\delta)$ decreases with δ and thus the FSLE analysis predicts an enhancement of the predictability time as observed in several numerical experiments.

We have illustrated these concepts on two model examples that possess different characteristic timescales.

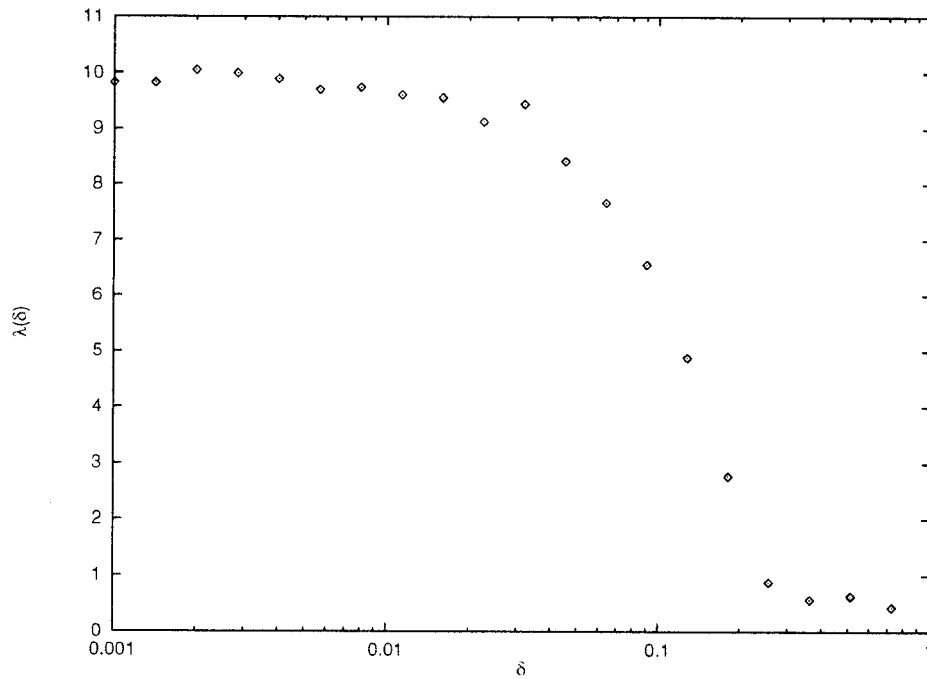


FIG. 5. FSLE computed for the toy atmospheric model. The parameters for the computation are: $\delta_0 = 10^{-3}$, $m = 20$, $r = 2^{1/2}$, and $N = 1000$.

The numerical computation of the FSLE confirms the predictability enhancement with respect to the Lyapunov analysis.

Our results have a general significance that exceeds

the proposed models. In particular, whenever one can identify in the system different features with different intrinsic timescales, one expects that slow varying quantities (i.e., large-scale features) are predictable longer

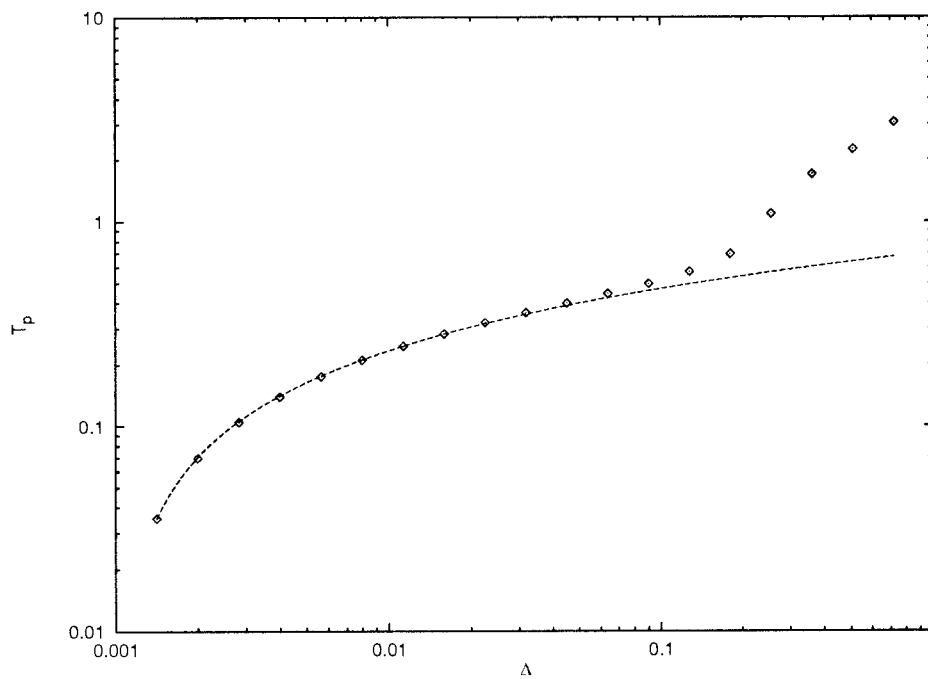


FIG. 6. Predictability time for the toy atmospheric model as a function of the tolerance Δ . The initial error is $\delta = 10^{-3}$. The dashed line represents the Lyapunov-based estimation.

than fast-evolving quantities. Moreover, our results suggest that the estimation of the large-scale predictability time in a general circulation model should not be affected too much by the particular small-scale parameterization.

Acknowledgments. This paper stems from the work of Giovanni Paladin, who has been tragically unable to see its conclusion. We dedicate it to his memory. G. Boffetta thanks the Istituto di Cosmogeofisica del CNR, Torino, for hospitality and support. This work has been partially supported by the CNR project, Climate Variability and Predictability.

REFERENCES

- Aurell, E., G. Boffetta, A. Crisanti, G. Paladin, and A. Vulpiani, 1996: Growth of non-infinitesimal perturbations in turbulence. *Phys. Rev. Lett.*, **77**, 1262–1265.
- , —, —, —, and —, 1997: Predictability in the large: An extension of the concept of Lyapunov exponent. *J. Phys.*, **A30**, 1–26.
- Benettin, G., L. Galgani, A. Giorgilli, and J. M. Strelcyn, 1980: Lyapunov characteristic exponent for smooth dynamical systems and Hamiltonian systems; a method for computing all of them. *Mechanica*, **15**, 9–20.
- Chen, W. Y., 1989: Estimate of dynamical predictability from NMC DERF experiments. *Mon. Wea. Rev.*, **117**, 1227–1236.
- Crisanti, A., M. H. Jensen, G. Paladin, and A. Vulpiani, 1993a: Predictability of velocity and temperature fields in intermittent turbulence. *J. Phys.*, **A26**, 6943–6960.
- , —, —, and —, 1993b: Intermittency and predictability in turbulence. *Phys. Rev. Lett.*, **70**, 166–169.
- Dalcher, A., and E. Kalnay, 1987: Error growth and predictability in operational ECMWF forecasts. *Tellus*, **39A**, 474–491.
- Eckmann, J. P., and D. Ruelle, 1985: Ergodic theory of chaos and strange attractors. *Rev. Mod. Phys.*, **57**, 617–656.
- Farrell, B. F., 1990: Small error dynamics and the predictability of atmospheric flows. *J. Atmos. Sci.*, **47**, 2409–2416.
- Gaspard, P., and X. J. Wang, 1993: Noise, chaos, and (ϵ, τ) -entropy per unit time. *Phys. Rep.*, **235**, 291–343.
- Leith, C. E., 1971: Atmospheric predictability and two-dimensional turbulence. *J. Atmos. Sci.*, **28**, 145–161.
- , 1975: Numerical weather prediction. *Rev. Geophys. Space Phys.*, **13**, 681–684.
- , 1978: Objective methods for weather prediction. *Annu. Rev. Fluid Mech.*, **10**, 107–128.
- , and R. H. Kraichnan, 1972: Predictability of turbulent flows. *J. Atmos. Sci.*, **29**, 1041–1058.
- Lorenz, E. N., 1963: Deterministic non-periodic flow. *J. Atmos. Sci.*, **20**, 130–141.
- , 1969: The predictability of a flow which possesses many scales of motion. *Tellus*, **21**, 289–307.
- , 1982: Atmospheric predictability experiments with a large numerical model. *Tellus*, **34**, 505–513.
- , 1996: Predictability—A problem partly solved. *Proc. Seminar on Predictability*. Reading, United Kingdom, European Centre for Medium-Range Weather Forecasts, 1–18.
- Simmons, A. J., R. Mureau, and T. Petroliaqis, 1995: Error growth and estimates of predictability from the ECMWF forecasting system. *Quart. J. Roy. Meteor. Soc.*, **121**, 1739–1771.
- Toth, Z., and E. Kalnay, 1993: Ensemble forecasting at NMC. *Bull. Amer. Meteor. Soc.*, **74**, 2317–2330.